

Article

Benchmarking Water-Use Efficiency for Wheat at Leaf and Ecosystem Scales

Funian Zhao ^{1,*}, Jiang Liu ^{2,*}, Qiang Zhang ¹, Liang Zhang ¹, Yue Qi ¹ and Fei Chen ¹ 

¹ Lanzhou Institute of Arid Meteorology, China Meteorological Administration, Key Laboratory of Arid Climatic Change and Disaster Reduction of Gansu Province, Key Laboratory of Arid Climate Change and Disaster Reduction of CMA, Lanzhou 730020, China; zhangqiang@cma.gov.cn (Q.Z.); zhangl@iamcma.cn (L.Z.); qiy@iamcma.cn (Y.Q.); chenf@iamcma.cn (F.C.)

² College of Resources and Environment, Gansu Agricultural University, Lanzhou 730070, China

* Correspondence: zhaofn@iamcma.cn (F.Z.); gauliujiang@163.com (J.L.); Tel.: +86-931-2402780 (F.Z.)

Abstract: The processes coupled with carbon and water exchange are linked to crop assimilation, water consumption, controlling crop growth and development, and ultimately determining crop yield. Therefore, studying the characteristics of crop water constraints and their controlling factors at multiple scales is of great significance for regional and global food production stability and food security. Employing field observations and a comprehensive literature review, this study investigates the maximum water-use efficiency of wheat and its governing factors at both leaf and canopy (ecosystem) scales. The results demonstrate remarkable consistency and well-defined boundaries in maximum water-use efficiency across diverse climate regions and wheat varieties, both at the leaf and agricultural ecosystem scales. At the leaf scale, the maximum water-use efficiency of wheat was $4.5 \mu\text{g C mg}^{-1} \text{H}_2\text{O}$, while for wheat agricultural ecosystems, on a daily scale, the maximum water-use efficiency was $4.5 \text{ g C kg}^{-1} \text{H}_2\text{O}$. Meanwhile, the maximum water-use efficiency of wheat agricultural ecosystems decreased continuously with increasing time scales, with values of 6.5, 4.5, 3.5, and $2 \text{ g C kg}^{-1} \text{H}_2\text{O}$ for instantaneous, daily, weekly, and monthly scales, respectively. Environmental factors, primarily vapor pressure deficit, light, and soil water content, exert significant control over leaf-level water-use efficiency. Similarly, the maximum water-use efficiency of agricultural ecosystems fluctuates in response to daily variations in meteorological elements. C3 crops like wheat exhibit remarkable resilience in their carbon–water exchange patterns across diverse environmental conditions. The findings in the current research can serve as a reference for improving crop water-use efficiency.

Keywords: water; leaf scale; canopy scale; maximum water-use efficiency; wheat



Citation: Zhao, F.; Liu, J.; Zhang, Q.; Zhang, L.; Qi, Y.; Chen, F. Benchmarking Water-Use Efficiency for Wheat at Leaf and Ecosystem Scales. *Atmosphere* **2024**, *15*, 163. <https://doi.org/10.3390/atmos15020163>

Academic Editor: Gianni Bellocchi

Received: 12 December 2023

Revised: 23 January 2024

Accepted: 24 January 2024

Published: 26 January 2024



Copyright: © 2024 by the authors. Licensee MDPI, Basel, Switzerland. This article is an open access article distributed under the terms and conditions of the Creative Commons Attribution (CC BY) license (<https://creativecommons.org/licenses/by/4.0/>).

1. Introduction

Agricultural production is influenced by various environmental factors such as light, temperature, water, fertility, and other management practices [1]. Globally, water deficit is the most significant environmental limiting factor for agricultural production [2,3]. Therefore, optimizing agricultural output under water scarcity has become a pressing imperative in ensuring global food security.

Water-use efficiency, which reflects the balance between crop output (generally referring to biomass accumulation or economic yield at the yield level, and carbon assimilation at the leaf and ecosystem scales) and water consumption, is often used to evaluate crop–water relationships at different spatial and temporal scales [4]. Due to its simple and easily understandable concept, water-use efficiency has been the focus of many researchers since the last century [5–7]. At the yield level, there has been a significant amount of research on crop water-use efficiency, and researchers have found that there is a benchmarking for water-use efficiency at the yield level [8], which means that, for the same crop, there should be an upper boundary, i.e., a maximum, for water-use efficiency at the yield level,

and this maximum converges globally. This indicates that the maximum water-use efficiency for the same crop tends to be similar worldwide. Moreover, some researchers have found that there is a similar maximum precipitation use efficiency under water-limited conditions for different ecosystems globally [9,10]. Crop yield and vegetation biomass formation are ultimately determined by carbon–water exchange at the leaf or ecosystem scales [11]. Therefore, the carbon–water coupling relationships at the leaf and ecosystem scales are crucial for analyzing crop or vegetation water relationships. However, there is currently insufficient research on the upper boundaries of water-use efficiency at the leaf or ecosystem scales for the same crop and it is still unclear whether there is a maximum water-use efficiency at both leaf and ecosystem scales for the same crop on a global scale.

At the leaf scale, the carbon–water exchange process is controlled by the opening and closing of stomata on the leaf surface [12], and there is a coupling relationship between the two processes. Therefore, changes in carbon–water exchange should be in a certain proportion and should not exceed a certain range. Limited water consumption can only fix a relative amount of carbon and cannot exceed a maximum value. Therefore, we infer that, at the leaf scale, the same crop should have an upper boundary for water-use efficiency. At the ecosystem scale, some studies have found that the carbon–water exchange of plants also follows a fixed proportion, with a linear relationship between transpiration and CO₂ flux (or net carbon exchange), similar to the relationship at the yield level [13,14]. Therefore, we have reason to believe that, at the ecosystem scale, the same crop may also have a similar maximum water-use efficiency.

However, at both leaf and ecosystem scales, changes in crop water-use efficiency occur at different time scales, and environmental factors vary at different time scales [15]. This raises the intriguing possibility of scale-specific convergence in crop maximum water-use efficiency, suggesting a unique optimal value for each temporal scale. However, considering the different environmental factors, biological and non-biological factors can cause changes in water-use efficiency, as water-use efficiency may vary with different time scales, such as daily or seasonal scales [16]. Therefore, it is necessary to understand the rules of water-use efficiency changes with time scales and their environmental controlling factors and further analyze the environmental background in which crop maximum water-use efficiency occurs.

Based on the initial product structure of the CO₂ fixation reaction, plants can be categorized into two main groups: C3 plants, which produce a three-carbon compound called 3-phosphoglycerate, and C4 plants, which synthesize a four-carbon product known as oxaloacetate [17]. In warmer climates with high yield potential, C4 photosynthesis is more efficient compared to C3 photosynthesis. Wheat is a typical C3 crop, and it is grown in different climatic regions worldwide due to its unique growth and development characteristics. Because C3 crops have typical photosynthetic physiology and are influenced by stomatal optimization [18], we speculate that crops like wheat should have similar maximum water-use efficiency at both leaf and ecosystem scales, and, with increasing time scale, the maximum water-use efficiency of wheat should decrease (other heterotrophic respiration processes will increase carbon assimilation consumption, leading to a decrease in water-use efficiency) [4].

This study aims to empirically validate the previously proposed hypothesis, elucidating the carbon–water coupling dynamics at various scales in wheat and the environmental factors regulating them. The objectives of this study are as follows: (1) to analyze and compare the maximum water-use efficiency of wheat at different spatial scales (leaf and ecosystem) and time scales (instantaneous, daily, weekly, and monthly); and (2) to determine the environmental factors that cause changes in water-use efficiency at different scales for wheat and analyze the environmental background in which the maximum water-use efficiency of wheat occurs. To address these objectives, we employed comprehensive data collection and analysis encompassing wheat leaves and field ecosystems across diverse climatic regions and observation areas, providing robust evidence to validate the hypothesized relationships.

2. Materials and Methods

2.1. Overview of Research Area and Experimental Design

This study analyzes the maximum water-use efficiency of wheat and its environmental influencing factors at two scales: leaf-level and farmland ecosystem scale. Field and pot experiments at the leaf level were conducted in the Dingxi Arid Meteorology and Ecological Environment Experimental Station affiliated with the Institute of Arid Meteorology (35°33' N, 104°35' E) (Figure 1). The station is located at an altitude of 1896.7 m with an annual average temperature of 7.1 °C, more than 2400 h of annual sunshine, an average annual precipitation of 386 mm, mostly concentrated in June to September accounting for 55.4% of the annual precipitation, and an average annual evaporation of 1500 mm. The frost-free period lasts for 140 days. This region falls within the category of a typical semi-arid climate zone.

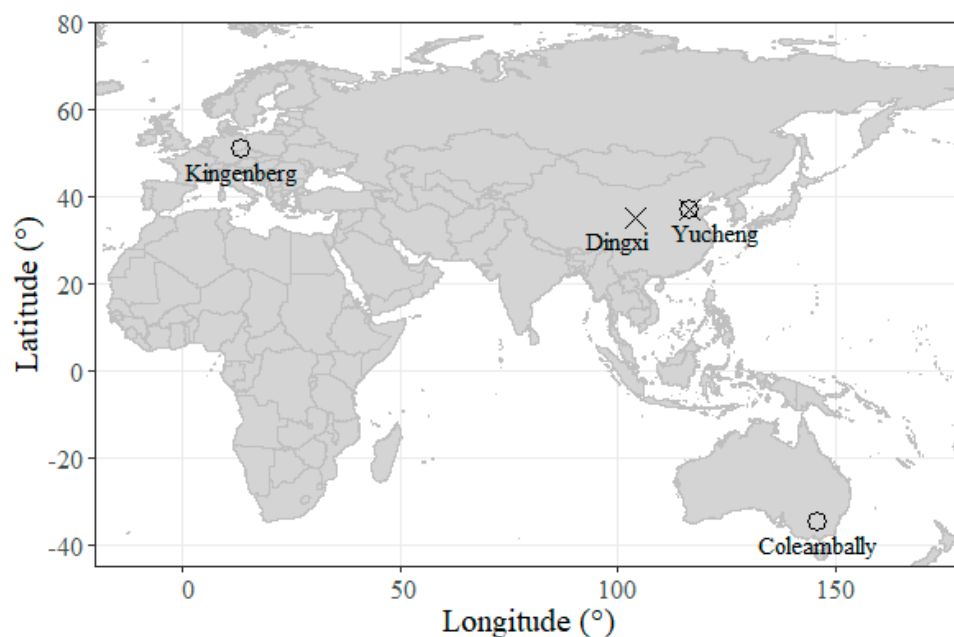


Figure 1. Observation sites of wheat gas exchange at leaf and ecosystem scales. 'x' represents the wheat leaf-level experimental observation site; 'o' represents the wheat ecosystem observation site.

The experimental crop for the trials was spring wheat, specifically the variety known as Dingxi New No. 24. Pot experiments were conducted in the years 2014, 2015, and 2017. The soil used for the experiments was loessial soil, collected from the 0–30 cm soil layer of the field, air-dried, sieved, and then placed in pots (with a diameter of 29 cm and a depth of 45 cm, with each pot containing 14 kg of soil). The average bulk density of the soil in the pots was 1.15 g cm^{-3} , with a field capacity of 26.8% and a wilting coefficient of 5.5%. Both field capacity and wilting coefficient represent weight-based soil moisture. For the 3-year experiment, 20 pots of wheat were planted each year. Out of these, 10 pots received ample water supply throughout the entire growth period (continuous watering), while the remaining 10 pots were subjected to drought conditions (given sufficient water from sowing until a specific growth stage, after which no further watering was provided, and natural rainfall was blocked). In the years 2014 and 2015, different experimental treatments commenced at the wheat jointing stage, while, in 2017, different treatments were applied during the flowering stage.

Field experiments were conducted in 2014 and 2017, with a wheat seeding density of 225 kg per hectare. In 2014, a randomized block design with four replicates per treatment was implemented. Two contrasting water regimes were established: (1) well-watered, ensuring ample water supply throughout the growing season, and (2) water-stressed, where irrigation was withheld from the wheat jointing stage until wilting symptoms appeared.

The plot size for each treatment in the 2014 experiment was 3.0 m² (2 m × 1.5 m). In 2017, 5 treatments were implemented, including no pre-sowing irrigation, irrigation of 10 mm, irrigation of 30 mm, irrigation of 60 mm, and irrigation of 90 mm (these treatments involved supplemental watering at different growth stages to maintain soil moisture content in the 100 cm soil layer above 75% of field capacity; when soil moisture fell below 75% of field capacity, additional watering was applied to reach 100% of field capacity). Each treatment had 4 replicates, and the plot size for the 2017 experiment was 3.0 m² (2 m × 1.5 m).

Some of the winter wheat leaf-level gas exchange experimental data were collected from observations at the Yucheng Experimental Station of the Chinese Academy of Sciences, located in the North China Plain (36°57' N, 116°36' E, at an elevation of 28 m) (Figure 1). The experiments at this station had only one treatment, which involved providing sufficient water throughout the entire winter wheat growth period. The wheat fields were well fertilized and irrigated routinely according to soil water content. Irrigation water of about 70–100 mm was applied 3 times after the turning-green stage. The detailed experimental management and environmental conditions at this station are referenced in [19].

Flux sites were selected from various climate zones to analyze the relationship between wheat yield and water availability in different climatic regions (Figure 1). The three selected sites were Kingenberg station (DE-Kli) in Europe, Germany (13°31' N, 50°54' E, at an elevation of 480 m) [20]; Yucheng station (YCS) in Asia, China (36°57' N, 116°36' E, at an elevation of 480 m) [21]; and Coleambally Wheat station in Oceania, Australia (34°8', 146°01', at an elevation of 120 m) [22]. Data from these three sites were obtained from the European Fluxes Database, ChinaFlux, and OzFlux, respectively. The climate types represented by these three sites are humid, semi-humid, and semi-arid, respectively. Typical years were chosen for wheat flux variation analysis. In the humid zone of Germany, data from 2005–2006 were selected for analysis, with wheat sown on 25 September 2005, and harvested on 26 September 2006. In the semi-humid zone of China, data from 2003–2004 were chosen for analysis, with wheat sown on 23 October 2003. In the semi-arid zone of Australia, data from 2011 were selected for analysis, with wheat sown on 6 May 2011, and harvested on 3 December 2011. The characteristic meteorological elements (temperature and saturation vapor pressure deficit) for these three sites in typical years are shown in Figure 2.

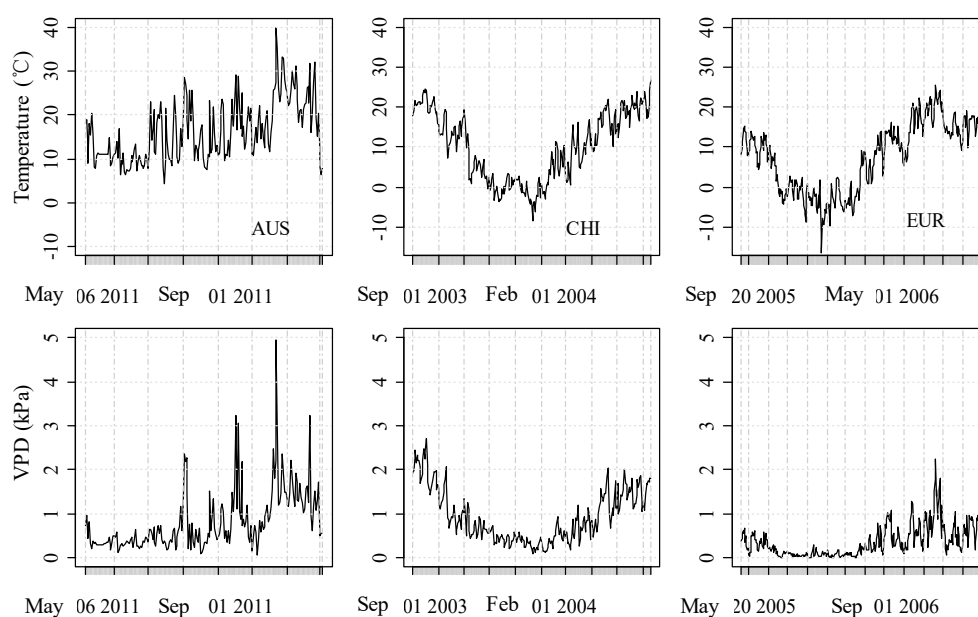


Figure 2. The seasonal variation of meteorological factors in three different observational sites. AUS represents the Coleambally Wheat station in New South Wales, Australia (2011). CHI represents the Yucheng station in Shandong, China (2004). EUR represents the Kingenberg station (DE-Kli) in Germany, Europe (2006).

2.2. The Experimental Observation Items and Methods

2.2.1. Leaf-Level Data Observation

1. Growth stages: detailed recording of the periods of crop growth and development. From seeding, emergence, three-leaf stage, seven-leaf stage, jointing, booting, heading (anthesis), flowering (silking), milk maturity, and maturity, observations were made when approximately 50% of the plants in each plot reached these developmental stages.

2. Soil moisture content (relative soil moisture throughout this paper): in potted experiments, the mass of 12 pots for each treatment was measured daily (with the smallest sensitivity of the used balance being 1 g). The soil moisture content in the pots was calculated by subtracting the dry soil weight from the measured weight and then dividing it by the dry soil weight (ignoring changes in wheat biomass). In field experiments, before water control, soil moisture content at depths of 0–100 cm in each experimental plot was measured every 20 cm at each growth stage. After the start of the controlled experiments, soil moisture content at depths of 0–100 cm in each experimental plot was measured every 5 days (every 10 cm) using soil augers, and the measurements were determined using the oven-drying method.

3. Diurnal variation in photosynthetic physiology: conducted during the wheat growth stages from jointing to flowering under clear weather conditions. Observations were made using a Li-6400 portable photosynthesis system with natural light as the source. During each observation, the first fully expanded leaf on the wheat canopy was selected for physiological parameter measurements. Observations were made every 2 h from 8:00 AM to 6:00 PM.

4. Light response curves and CO₂ response curves for photosynthesis. utilized a Li-6400 portable photosynthesis system produced in the United States. During the spring wheat growth stage from jointing onward and after implementing different experimental treatments, photosynthesis vs. quantum photosynthetic flux density (Pn/Qp, light response) and photosynthesis vs. intercellular CO₂ concentration (Pn/Ci, CO₂ response) curves were measured daily from 9:00 AM to 11:30 AM (Pn/Qp curves were primarily measured in 2014 and 2015, while Pn/Ci curves were primarily measured in 2017). For Pn/Qp curve measurements, the controlled CO₂ concentration was 380 μmol·mol⁻¹, leaf chamber temperature was maintained at 25 °C, and vapor pressure deficit was controlled between 1.5 and 2.5 kPa. Measurements were taken using a red–blue light source, and photosynthetically active radiation (PAR) was automatically measured at different gradients: 0, 15, 30, 60, 120, 200, 300, 600, 900, 1200, 1500, 1800, and 2100 μmol m⁻² s⁻¹. Each measurement included a 30–40-min adaptation period at 1500 μmol m⁻² s⁻¹ PAR, and once the instrument readings stabilized, automatic measurements were initiated. For Pn/Ci curve measurements, the initial CO₂ concentration was controlled at 380 μmol mol⁻¹, leaf chamber temperature at 25 °C, and vapor pressure deficit between 1.5 and 2.5 kPa. Light intensity was controlled at 1500 μmol m⁻² s⁻¹, and, before starting measurements, an initial adaptation period of 30–40 min was applied under initial conditions. CO₂ gradients were set at 400, 200, 100, 50, 400, 600, 800, 1000, and 1200 μmol mol⁻¹, and measurements were made automatically. While observing leaf gas exchange, the Li-6400 also recorded meteorological parameters such as leaf chamber air temperature, relative humidity, leaf–air temperature difference, leaf–air saturation vapor pressure difference, and air CO₂ concentration.

2.2.2. Leaf Exchange Data from Literature

The literature data were sourced from the global plant stomatal behavior database collected and compiled by Lin et al. (2015) [23]. This study selected datasets of C3 crops in humid and semi-arid regions, mainly including crop stomatal conductance, net photosynthesis rate, leaf temperature, air CO₂ concentration, and vapor pressure deficit.

2.2.3. Flux Data Observation and Processing

The flux data primarily include ecosystem net exchange (NEE), latent heat flux (LE), air temperature (Ta), photosynthetically active radiation (PAR), precipitation (P), and satu-

ration vapor pressure deficit (etc.). NEE and LE are both obtained through flux observations using the eddy covariance system, with a sampling frequency of 10 Hz at all three stations and an observation time interval of 30 min. Other meteorological data were also observed at 30 min intervals. Missing values and outliers in the flux observations were supplemented using linear interpolation based on data before and after the observation, and daily, weekly, monthly, and growing season values were obtained through accumulation. The wheat field ecosystem's water consumption (ET) was calculated from latent heat as $ET = LE/\gamma$, where γ represents the latent heat of water with a value of 2.26 MJ kg^{-1} .

2.3. The Calculation Method for Water-Use Efficiency (WUE)

This study involves two different scales of wheat carbon exchange. At the leaf scale, water-use efficiency (WUE_i) is defined as the ratio of net photosynthesis rate (P_n) to transpiration rate (Tr):

$$WUE_i = \frac{P_n}{Tr} \quad (1)$$

At the ecosystem scale, water-use efficiency (WUE) is calculated using net ecosystem productivity (NEP, also known as $-NEE$), defined as

$$WUE = \frac{NEP}{ET} = \frac{-NEE}{ET} \quad (2)$$

At the leaf scale, the unit of WUE_i is $\mu\text{g C mg}^{-1} \text{ H}_2\text{O}$, calculated from leaf-scale observational data by multiplying P_n by 12, the molecular weight of carbon, and Tr by 18, the molecular weight of water, as per Equation (1).

At the agroecosystem scale, instantaneous WUE is expressed in units of $\mu\text{g C mg}^{-1} \text{ H}_2\text{O}$, while daily, weekly, and monthly WUE are measured in units of $\text{g C kg}^{-1} \text{ H}_2\text{O}$. Daily, weekly, and monthly NEE and ET (evapotranspiration) data are cumulatively derived from half-hourly instantaneous observations.

3. Results

3.1. The Consistency of Leaf-Scale Observations across Different Observation Times, Water Stress Levels, and Climate Zones

Analyzing wheat water-use efficiency under different temperatures, varying moisture supply conditions, different observation periods, and various climate zones (Figure 3), we observed that, despite differences in meteorological conditions, moisture availability, observation times, and climatic backgrounds, the maximum leaf-scale water-use efficiency of wheat under different environmental conditions approached consistency, with values converging around $4.5 \mu\text{g C mg}^{-1} \text{ H}_2\text{O}$.

In Figure 3a, it is shown that under moderate to cool temperature conditions, wheat leaf-scale water-use efficiency is more likely to reach its maximum value, while light intensity appears to have no significant impact on the occurrence of maximum water-use efficiency. In comparison to regions with higher moisture levels, semi-arid areas show that crops like wheat tend to achieve maximum water-use efficiency more readily (Figure 3b). Furthermore, during the morning hours of the day, wheat leaf-scale water-use efficiency is closer to its maximum value, decreasing during midday and afternoon, with the lowest values occurring at noon (Figure 3c). Additionally, as seen in Figure 3d, under well-supplied moisture conditions, wheat transpiration increases, while water-use efficiency decreases. Conversely, under moisture stress conditions, wheat leaf-scale water-use efficiency is more likely to reach its maximum value.

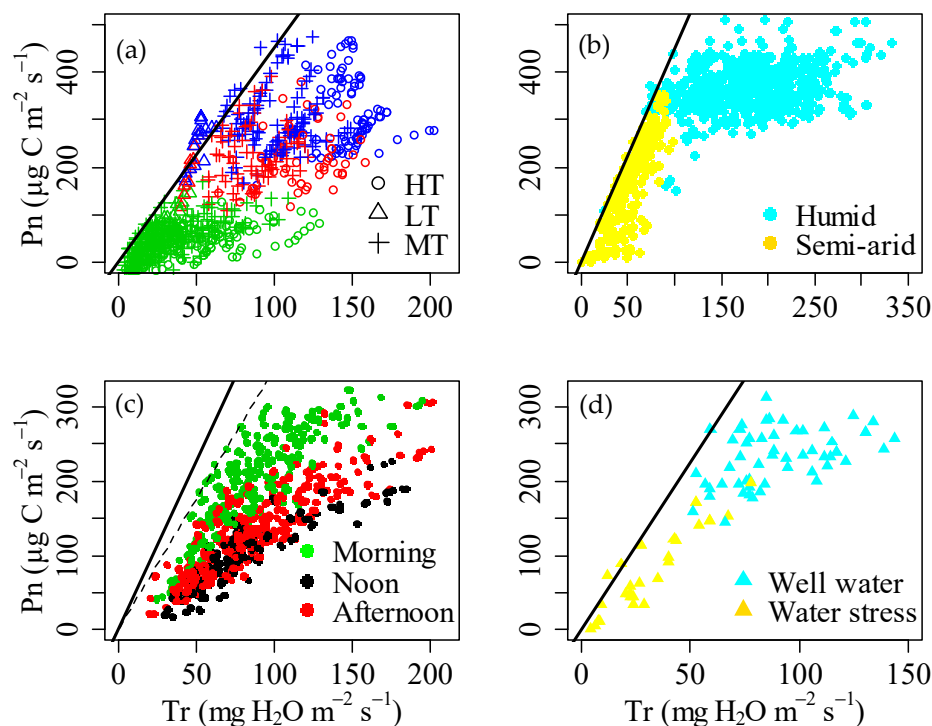


Figure 3. The relationship between net photosynthesis rate and transpiration rate at leaf scale for wheat under different environmental conditions. The solid black line represents the maximum potential water-use efficiency: $P_n = 4.5 \mu\text{g C mg}^{-1} \text{H}_2\text{O Tr}$. (a) Winter wheat indices under different light (green weak light, red moderate light, blue high light) and temperature (LT low-temperature range, MT intermediate temperature range, HT high-temperature range) conditions; (b) leaf gas exchange of crops in global humid and semi-arid regions collected by Lin et al. (2015) [23] (crops in semi-arid regions are wheat, and, in humid regions, cotton and buckwheat); (c) spring wheat leaf indices under diurnal conditions; (d) spring wheat leaf indices under different water treatments, with controlled light intensity, temperature, and CO_2 conditions.

3.2. Analysis of Leaf-Scale Influencing Factors

3.2.1. The Influence of Light and Temperature

Analyzing the relationship between vapor pressure deficit and temperature, it was found that they exhibit an exponential relationship, with higher temperatures corresponding to greater vapor pressure deficit (Figure omitted). This corresponds to the growth environment of spring wheat and winter wheat, where the relationship between air saturation and temperature is in line with this observation, with higher temperatures corresponding to higher vapor pressure deficit and lower temperatures corresponding to smaller vapor pressure deficit (Figure 4a,c). Furthermore, within the same temperature range, it is shown that stronger radiation leads to a smaller vapor pressure deficit. When examining the variations in water-use efficiency of different wheat leaf types under different lighting and temperature conditions (Figure 4b,d), it is evident that, within the same range of radiation changes, lower temperatures result in higher leaf-scale water-use efficiency for both wheat types. Additionally, within the same temperature range, stronger radiation leads to higher water-use efficiency for wheat. Whether it is winter wheat or spring wheat, the maximum leaf water-use efficiency occurs within the range of meteorological factors characterized by higher radiation and lower temperatures. It can also be noted that, regardless of the temperature change range, higher radiation always corresponds to greater water-use efficiency in wheat.

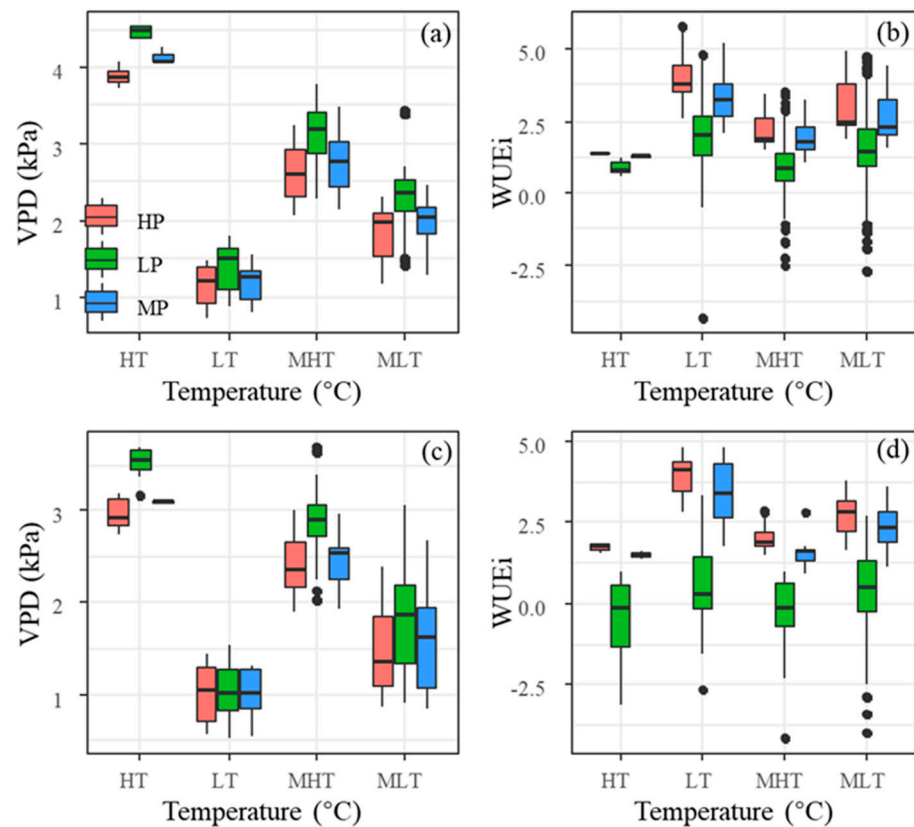


Figure 4. The variation of vapor pressure deficit and water-use efficiency for wheat under different temperature and radiation conditions. (a,b) Represent winter wheat, while (c,d) represent spring wheat. HT stands for temperatures greater than 32 °C, MHT represents temperatures between 28 and 32 °C, MLT represents temperatures between 22 and 28 °C, and LT represents temperatures below 22 °C. HP represents radiation greater than 950 $\mu\text{mol m}^{-2} \text{s}^{-1}$, MP represents radiation between 300 and 950 $\mu\text{mol m}^{-2} \text{s}^{-1}$, and LP represents radiation less than 300 $\mu\text{mol m}^{-2} \text{s}^{-1}$. WUEi is measured in units of $\mu\text{g C mg}^{-1} \text{H}_2\text{O}$. VPD indicates vapor pressure deficit.

3.2.2. The Influence of Vapor Pressure Deficit

Observing the relationships between various leaf gas exchange parameters of spring wheat and vapor pressure deficit (Figure 5a), it is observed that, as vapor pressure deficit increases, stomatal conductance decreases, showing an inverse relationship between the two. The net photosynthetic rate initially stabilizes and then decreases rapidly with increasing vapor pressure deficit (Figure 5b). The transpiration rate remains stable initially with changes in vapor pressure deficit (Figure 5c) and then increases with increasing vapor pressure deficit. However, once the vapor pressure deficit exceeds 3 kPa, further increases in vapor pressure deficit lead to a rapid reduction in transpiration rate, indicating a threshold response of transpiration rate to changes in vapor pressure deficit. Wheat leaf water-use efficiency initially stabilizes and then rapidly decreases with increasing vapor pressure deficit, with its pattern of change closely resembling the relationship between net photosynthetic rate and vapor pressure deficit (Figure 5d). The maximum water-use efficiency of spring wheat occurs under conditions of lower vapor pressure deficit, meaning that when the vapor pressure deficit is lower, the water-use efficiency of spring wheat is relatively higher.

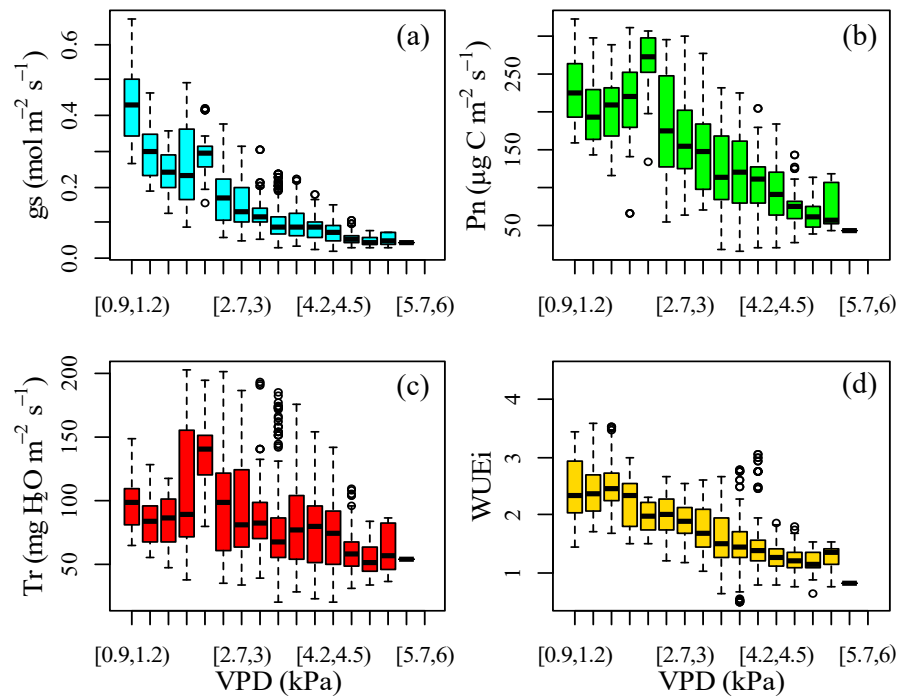


Figure 5. The response of leaf gas exchange parameters, including (a) stomatal conductance (g_s), (b) photosynthetic rate (P_n), (c) transpiration rate (T_r) and (d) water-use efficiency (WUE_i) to vapor pressure deficit (VPD). The unit of WUE_i is $\mu\text{g C mg}^{-1} \text{H}_2\text{O}$.

3.2.3. The Influence of Soil Water

Examining the leaf-scale gas exchange parameters of field-grown and potted wheat under varying moisture conditions in Figures 6 and 7 reveals a consistent decline in stomatal conductance as moisture supply diminishes. Due to strict experimental control conditions, there is no clear pattern in the variation of vapor pressure deficit, or vapor pressure deficit only shows slight increases with decreasing soil moisture, but the average values do not exceed 3 kPa (Figures 6a and 7a).

Observing the changing relationship between moisture supply conditions and water-use efficiency, it is found that the data obtained from the field experiments show that as moisture supply decreases, leaf-scale water-use efficiency initially stabilizes and then increases continuously. However, with further reduction in moisture supply, water-use efficiency decreases rapidly (Figure 6d). In potted experiments, the drought process occurs more rapidly, and the data are relatively sparse. Still, careful observation reveals a similar relationship between leaf-scale water-use efficiency and moisture supply conditions, where water-use efficiency slowly increases and then rapidly decreases with decreasing moisture supply (Figure 7d).

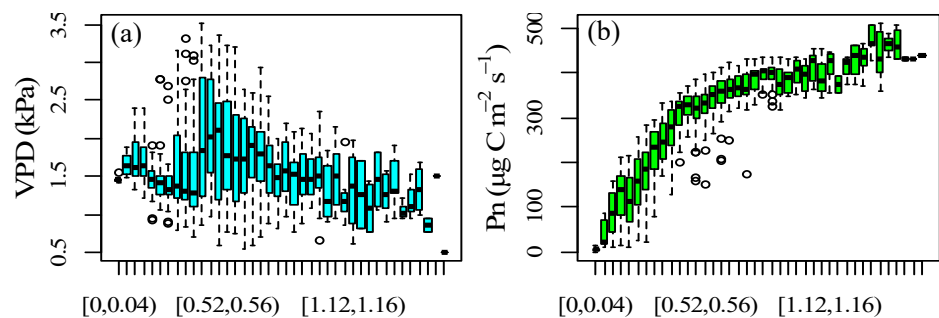


Figure 6. Cont.

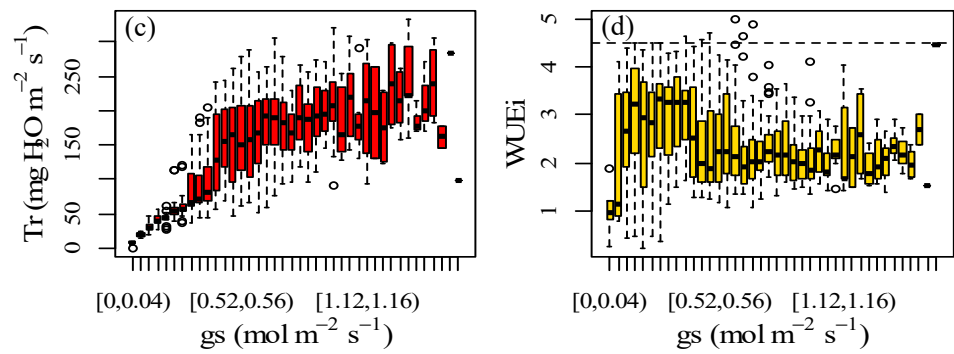


Figure 6. The response of leaf gas exchange parameters, including (a) vapor press deficit (VPD), (b) photosynthetic rate (Pn), (c) transpiration rate (Tr) and (d) water-use efficiency (WUEi) to stomatal conductance (gs) for wheat growing in field to different water conditions. The unit of WUEi is $\mu\text{g C mg}^{-1} \text{H}_2\text{O}$.

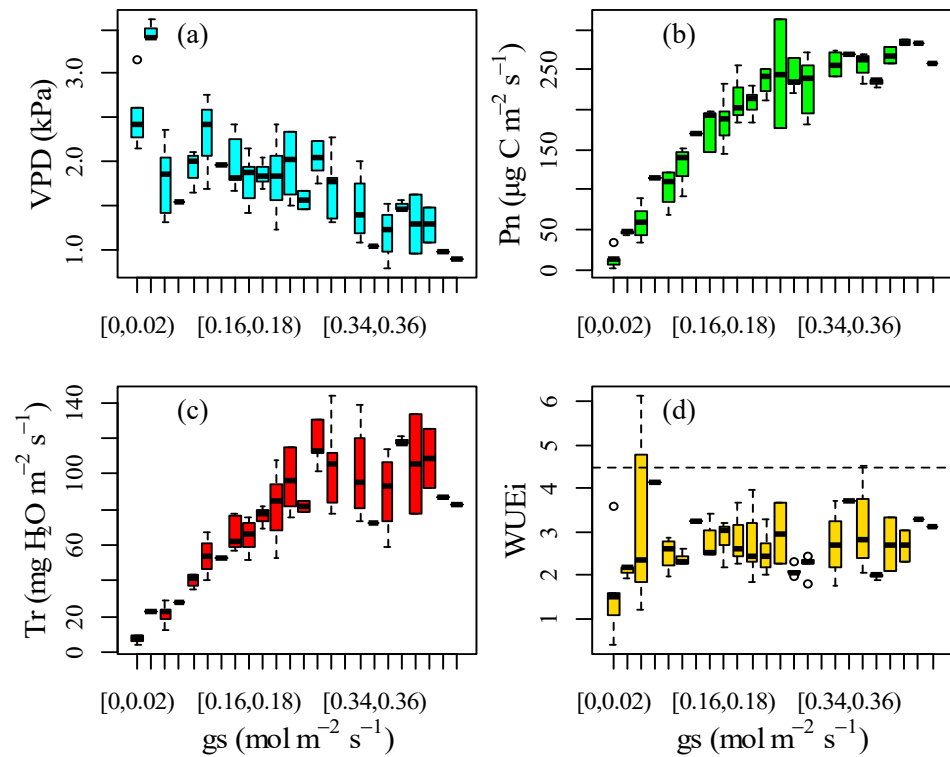


Figure 7. The response of leaf gas exchange parameters, including (a) vapor press deficit (VPD), (b) photosynthetic rate (Pn), (c) transpiration rate (Tr) and (d) water-use efficiency (WUEi) to stomatal conductance (gs) for wheat growing in pot to different water conditions. The unit of WUEi is $\mu\text{g C mg}^{-1} \text{H}_2\text{O}$.

3.3. Maximum Water-Use Efficiency of Wheat Agroecosystems at Different Time Scales in Various Climatic Regions

3.3.1. Different Temporal Scales

Analyzing the relationship of carbon–water exchange in wheat agroecosystems across different climatic regions (Figure 8), it is observed that, despite varying climatic backgrounds, the maximum water-use efficiency in different climatic regions tends to converge over different time scales. At the daily time scale, the maximum water-use efficiency at all three sites is approximately $4.5 \text{ g C kg}^{-1} \text{H}_2\text{O}$ (Figure 8a), with each site showing water-use efficiency values reaching or approaching $4.5 \text{ g C kg}^{-1} \text{H}_2\text{O}$. However, it is worth noting that the site located in the humid region exhibits a relatively higher frequency of maximum values.

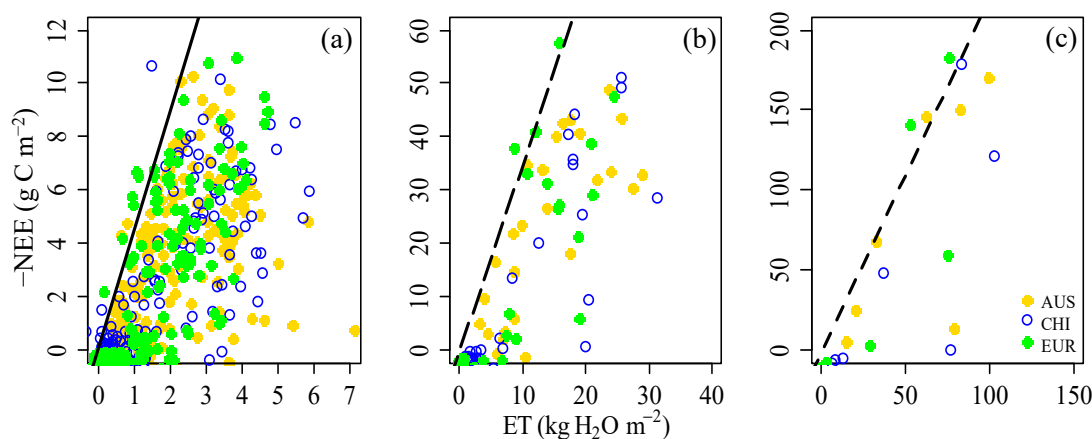


Figure 8. The response of net carbon exchange to evapotranspiration for wheat in different stations with different climates. (a) For the daily scale, (b) for the weekly scale, and (c) for the monthly scale. AUS represents Coleambally Wheat station in New South Wales, Australia (2011), CHI represents Yucheng station in Shandong, China (2004), and EUR represents Kingenberg (DE-Kli) in Germany, Europe (2006). The black diagonal lines represent the maximum potential water-use efficiency, which is $4.5 \text{ g C kg}^{-1} \text{ H}_2\text{O}$ on the daily scale, $3 \text{ g C kg}^{-1} \text{ H}_2\text{O}$ on the weekly scale, and $2.2 \text{ g C kg}^{-1} \text{ H}_2\text{O}$ on the monthly scale.

At the weekly time scale (Figure 8b), the maximum water-use efficiency at all three sites converges to around $3 \text{ g C kg}^{-1} \text{ H}_2\text{O}$, while at the monthly time scale, it is approximately $2.2 \text{ g C kg}^{-1} \text{ H}_2\text{O}$ (Figure 8c). At both the weekly and monthly time scales, sites in humid climatic regions also show a relatively higher frequency of water-use efficiency values reaching or approaching the maximum.

3.3.2. Water-Use Efficiency Variations at the Half-Hour Scale

On the half-hour scale, the maximum water-use efficiency in wheat field ecosystems at three different climatic zones tends to be consistent, but it is significantly influenced by the time of day (Figure 9). During the morning period, the maximum value is $11.5 \mu\text{g C mg}^{-1} \text{ H}_2\text{O}$, while at noon, it is $4.5 \mu\text{g C mg}^{-1} \text{ H}_2\text{O}$, and during the afternoon, it is $6.5 \mu\text{g C mg}^{-1} \text{ H}_2\text{O}$. However, when observing the data for the entire growth period, it is evident that, at various sites, there are many instances where water-use efficiency exceeds the given maximum water-use efficiency (Figure 9a–c). Yet, when examining the data for the peak growth period (the main growth period), it becomes apparent that the specified maximum water-use efficiency serves as a boundary for water-use efficiency across different time periods (Figure 9d–f).

Data collected throughout the wheat growth period are susceptible to influences from various observation-related factors, particularly during the early and late stages. During these stages, wheat growth may not completely cover the ground, or wheat may age, resulting in a decrease in leaf area index. The presence of exposed soil can impact variations in evapotranspiration, and the observed field water exchange is not solely due to wheat transpiration but also includes some direct soil evaporation. This can lead to momentary and drastic fluctuations in water-use efficiency in wheat field ecosystems, potentially causing some observational data to exceed the specified maximum water-use efficiency.

During the peak growth period, when the aboveground portion of wheat fully covers the soil, the water exchange in the field ecosystem can substitute for wheat transpiration. Consequently, during this period, the data exhibit a clear boundary and distribution pattern.

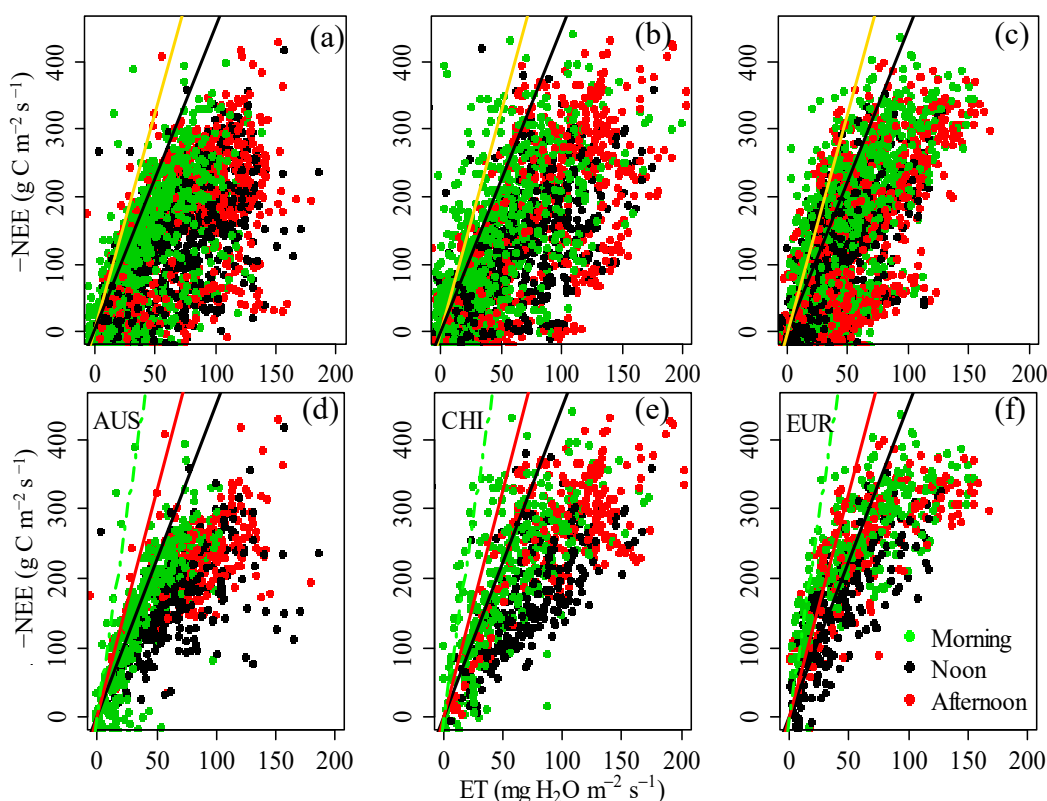


Figure 9. The response of seasonal and main seasonal net carbon exchange to evapotranspiration for wheat at different stations with different climates. (a,d) Coleambally Wheat station in New South Wales, Australia (2011), (b,e) Yucheng station in Shandong, China (2004), and (c,f) Kingenberg (DE-Kli) station in Germany, Europe (2006). The green diagonal line represents a maximum potential water-use efficiency of $11.5 \mu\text{g C mg}^{-1} \text{H}_2\text{O}$, the red and orange diagonal line represents a maximum potential water-use efficiency of $6.5 \mu\text{g C mg}^{-1} \text{H}_2\text{O}$, and the black line represents a maximum potential water-use efficiency of $4.5 \mu\text{g C mg}^{-1} \text{H}_2\text{O}$.

3.3.3. The Variation of Maximum Water-Use Efficiency at the Daily Scale in Wheat Agroecosystems during Different Growth Stages

Analyzing the variation of maximum water-use efficiency on the daily scale in wheat agroecosystems across different climatic stations during various growth stages (Figure 10), it was observed that, during the mid-growth stage, wheat agroecosystems tend to achieve higher water-use efficiency. However, in the later stages of growth, there is a significant reduction in water-use efficiency within wheat agroecosystems, indicating a notable impact of direct soil evaporation on water-use efficiency. This is attributed to the larger leaf area index of wheat during the mid-growth stage (Figure 11b, for humid region stations), which implies less exposed bare soil. As the wheat leaves start to senesce in the later stages (Figure 11c,d, for humid region stations), a substantial amount of soil becomes exposed on the surface. Consequently, the proportion of water loss through wheat transpiration in total field evapotranspiration decreases gradually. Furthermore, as the wheat enters the late growth stage, during the peak summer season, the elevated atmospheric temperatures lead to increased atmospheric evaporative demand, resulting in a rapid increase in direct soil evaporation. In this stage, wheat agroecosystems experience significant inefficient water loss within field evapotranspiration, as senescent wheat leaves are unable to assimilate a substantial amount of dry matter. Consequently, water-use efficiency in the field decreases rapidly.

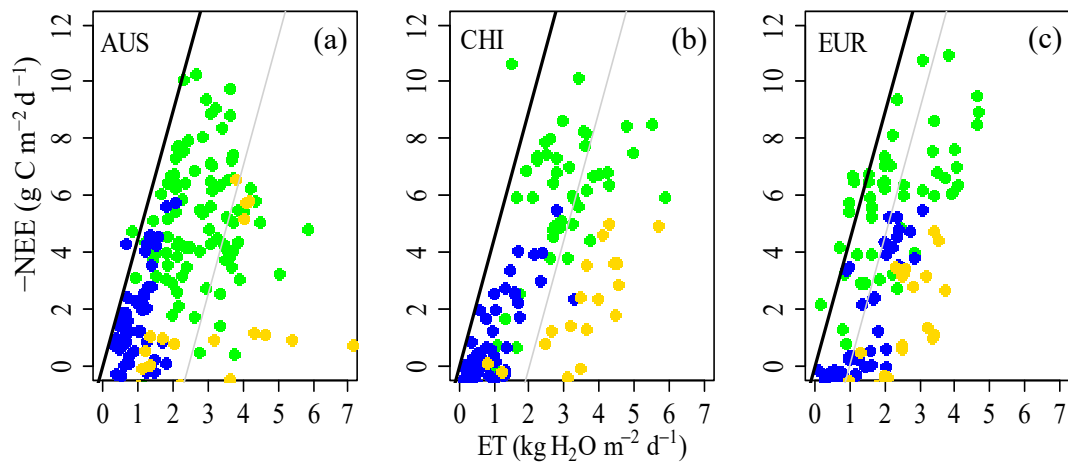


Figure 10. The response of daily net carbon exchange to evapotranspiration for wheat at different stations with different climates. (a) Coleambally Wheat station in New South Wales, Australia (2011), (b) Yucheng station in Shandong, China (2004), and (c) Kingenberg (DE-Kli) station in Germany, Europe (2006). The black and grey line represents the maximum potential water-use efficiency of $4.5 \text{ mg C kg}^{-1} \text{ H}_2\text{O}$ with and without soil evaporation. Blue dots indicate the early growth stage, green dots represent the mid-growth stage, and gold dots denote the late growth stage.

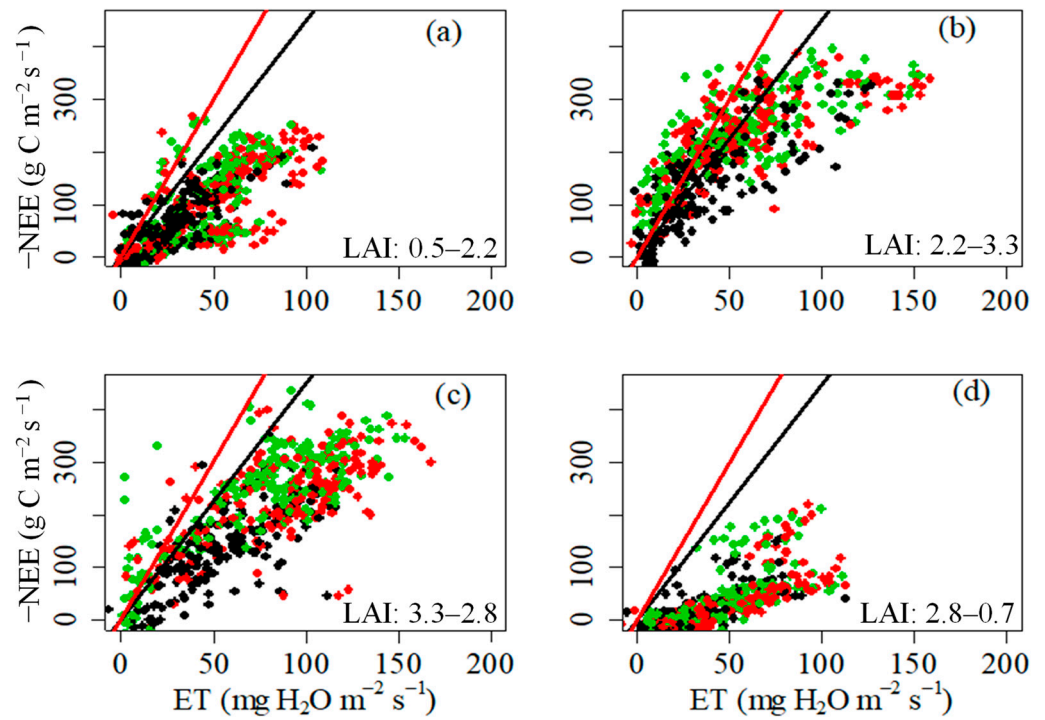


Figure 11. The response of hourly net carbon exchange to evapotranspiration for wheat during different growing stages under humid climate. (a) Early growing season with leaf area index from 0.5 to 2.2. (b) Middle growing season with leaf area index from 2.2 to 3.3. (c) Middle late growing season with leaf area index from 3.3 to 2.8. (d) Late growing season with leaf area index from 2.8 to 0.7. Green dots represent morning data, black dots represent noon data, and red dots represent afternoon data. The red diagonal line represents a maximum potential water-use efficiency of $6.5 \text{ } \mu\text{g C mg}^{-1} \text{ H}_2\text{O}$, while the black line represents a maximum potential water-use efficiency of $4.5 \text{ } \mu\text{g C mg}^{-1} \text{ H}_2\text{O}$. LAI indicates leaf area index.

4. Discussion

This study investigates the existence of a maximum water-use efficiency for wheat at both the leaf and ecosystem scales, essentially testing for a conservative trade-off between its productivity and water consumption across these levels. Through the analysis presented in this article, it is found that, consistent with relationships between water and crops observed in various ecosystems, precipitation levels, and yield levels [8,9], wheat also exhibits an upper boundary in water-use efficiency at both the leaf and ecosystem scales. Crop assimilation processes are regulated by the opening and closing of stomata [24], and during the process of crop photosynthesis where CO₂ is absorbed, there is inevitably an accompanying transpiration water consumption process. Therefore, water-use efficiency essentially represents a balance between crop yield and water consumption [18]. Consequently, with limited water supply, crop yield is bound to vary proportionally within a certain range. This explains why, whether at the leaf, ecosystem, or yield levels, there exists a maximum water-use efficiency, or in other words, an upper boundary.

At the leaf scale, the maximum water-use efficiency of wheat is 4.5 $\mu\text{g C mg}^{-1} \text{H}_2\text{O}$. However, at the agroecosystem scale, the maximum water-use efficiency of wheat varies between 20 and 11.5 $\text{mg C kg}^{-1} \text{H}_2\text{O}$ (across multiple time scales), while at the daily scale, it is 4.5 $\text{mg C kg}^{-1} \text{H}_2\text{O}$. After unit conversion, its value is similar to the maximum water-use efficiency at the leaf scale.

Observing the changes in leaf area index (LAI) in the wheat agroecosystem with the growth stages in Figure 11, it can be seen that, during the peak growth stage, the wheat LAI exceeds 3, indicating complete ground coverage by wheat in the field. In such cases, the wheat canopy can be treated as a single large leaf, and due to its vertical structure, the assimilation and transpiration processes within the wheat canopy are more pronounced than in individual leaves. Consequently, at the agroecosystem scale, it is plausible for wheat to exhibit maximum water-use efficiency that surpasses or approximates the leaf-scale maximum throughout the growth period.

The main factors influencing the attainment of maximum water-use efficiency in crops at the yield level include atmospheric evaporation, water stress during critical growth stages, soil fertility, as well as weed and pest pressures [25–27]. These factors similarly impact the variation in wheat water-use efficiency at both the leaf and ecosystem scales. Furthermore, considering the temporal changes in environmental factors on scales such as instantaneous, daily, weekly, and monthly, changes in water-use efficiency at the leaf and ecosystem scales are also significantly influenced by factors such as temperature, light exposure, and vapor pressure deficit.

The optimal temperature range for wheat growth and development falls between 19 and 23 °C [28]. Relatively lower temperatures favor photosynthesis in wheat, consequently improving water-use efficiency (Figure 4). Additionally, a lower vapor pressure deficit promotes the opening of wheat leaf stomata, allowing wheat to achieve greater yields at lower transpiration rates. This explains why water-use efficiency is relatively higher in the morning for both leaves and agroecosystems (Figures 3 and 9).

The current research results indicate that moderate water deficit is beneficial for improving crop water-use efficiency [29], which also confirms the applicability of deficit irrigation in irrigated agricultural areas. However, it is necessary to note that reducing crop water supply to a certain extent comes at the cost of reducing assimilate accumulation. Therefore, it is also important to consider how to achieve maximum crop yield under limited water supply conditions.

5. Conclusions

Wheat exhibits boundaries in its carbon–water relationships at different spatiotemporal scales, with water-use efficiency displaying convergence. At the leaf scale, the instantaneous maximum water-use efficiency for wheat is 4.5 $\mu\text{g C mg}^{-1} \text{H}_2\text{O}$, while, at the agroecosystem scale, the maximum water-use efficiency ranges from 2.2 to 11.5 mg C kg^{-1}

H₂O at different temporal scales. As the temporal scale increases, the maximum water-use efficiency of wheat agroecosystems gradually decreases.

At the leaf scale, the primary factors influencing wheat's carbon–water relationships, namely water-use efficiency, are vapor pressure deficit, temperature, light, and soil moisture, with CO₂ also playing a role (not discussed in this study, which solely considers current climate scenarios). At the wheat agroecosystem scale, in addition to the aforementioned environmental factors, variations in LAI also impact the changes in wheat water-use efficiency.

Crops or plants have the maximum water-use efficiency for better water use under different conditions considering the relationships between assimilation and water use. The benchmark for water-use efficiency in the current analysis could be used as potential water-use efficiency, and the gaps among these different water-use efficiency levels and the most limiting factors to the gaps were identified for possible improvements in water-use efficiency.

Author Contributions: Conceptualization, F.Z. and Q.Z.; methodology, F.Z.; software, J.L.; validation, L.Z., F.Z. and Q.Z.; formal analysis, F.Z.; investigation, F.Z.; resources, F.C.; data curation, Y.Q.; writing—original draft preparation, F.Z.; writing—review and editing, Q.Z.; visualization, Y.Q.; supervision, Q.Z.; project administration, Q.Z.; funding acquisition, Q.Z. All authors have read and agreed to the published version of the manuscript.

Funding: This research was funded by the National Natural Science Foundation of China (42230611, 42005097, 42175192), Joint Research Project for Enhancing Meteorological Capabilities by the China Meteorological Administration (23NLTSZ008), Natural Science Foundation of Gansu Province (23JRRJ0005), and Postdoctoral Research Fund Project (BSH2022001).

Institutional Review Board Statement: Not applicable.

Informed Consent Statement: Not applicable.

Data Availability Statement: The data presented in this study are available on request from the corresponding author. The data are not publicly available due to privacy.

Acknowledgments: The tower flux data used for this study were obtained from the fluxnet (<https://fluxnet.org/>, accessed on 23 January 2024), ChinaFlux (<http://www.chinaflux.org/enn/index.aspx>, accessed on 23 January 2024), and OzFlux (<https://www.ozflux.org.au/>, accessed on 23 January 2024) networks. We acknowledge the three sites used in the current study for their data records. The authors sincerely thank the anonymous reviewers for their valuable comments and suggestions for improving the quality of this paper. The authors also gratefully acknowledge the help of Quanyao Fang for his comments on the first draft of this manuscript.

Conflicts of Interest: The authors declare no conflict of interest.

References

1. Maestrini, B.; Basso, B. Predicting spatial patterns of within-field crop yield variability. *Field Crops Res.* **2018**, *219*, 106–112. [[CrossRef](#)]
2. Mbava, N.; Mutema, M.; Zengeni, R.; Shimelis, H.; Chaplot, V. Factors affecting crop water use efficiency: A worldwide meta-analysis. *Agric. Water Manag.* **2020**, *228*, 105878. [[CrossRef](#)]
3. Nechifor, V.; Winning, M. Global crop output and irrigation water requirements under a changing climate. *Heliyon* **2019**, *5*, e01266. [[CrossRef](#)]
4. Tallec, T.; Béziat, P.; Jarosz, N.; Rivalland, V.; Ceschia, E. Crops' water use efficiencies in temperate climate: Comparison of stand, ecosystem and agronomical approaches. *Agric. For. Meteorol.* **2013**, *168*, 69–81. [[CrossRef](#)]
5. Bchir, A.; Escalona, J.M.; Galle, A.; Hernandez-Montes, E.; Tortosa, I.; Brahama, M.; Medrano, H. Carbon isotope discrimination ($\delta^{13}C$) as an indicator of vine water status and water use efficiency (WUE): Looking for the most representative sample and sampling time. *Agric. Water Manag.* **2016**, *167*, 11–20. [[CrossRef](#)]
6. Medrano, H.; Tomás, M.; Martorell, S.; Flexas, J.; Hernández, E.; Rosselló, J.; Pou, A.; Escalona, J.M.; Bota, J. From leaf to whole-plant water use efficiency (WUE) in complex canopies: Limitations of leaf WUE as a selection target. *Crop J.* **2015**, *3*, 220–228. [[CrossRef](#)]
7. Gao, H.H.; Yan, C.R.; Liu, Q.; Li, Z.; Yang, X.; Qi, R.M. Exploring optimal soil mulching to enhance yield and water use efficiency in maize cropping in China: A meta-analysis. *Agric. Water Manag.* **2019**, *225*, 105741. [[CrossRef](#)]

8. Sadras, V.O.; Angus, J.F. Benchmarking water-use efficiency of rainfed wheat in dry environments. *Aust. J. Agric. Res.* **2006**, *57*, 847–856. [[CrossRef](#)]
9. Huxman, T.E.; Smith, M.D.; Fay, P.A.; Knapp, A.K.; Shaw, M.R.; Loik, M.E.; Smith, S.D.; Tissue, D.T.; Zak, J.C.; Weltzin, J.F.; et al. Convergence across biomes to a common rain-use efficiency. *Nature* **2004**, *429*, 651–654. [[CrossRef](#)]
10. Knapp, A.K.; Burns, C.E.; Fynn, R.W.S.; Kirkman, K.P.; Morris, C.D.; Smith, M.D. Convergence and contingency in production–precipitation relationships in North American and South African C4 grasslands. *Oecologia* **2006**, *149*, 456–464. [[CrossRef](#)]
11. Ferraz, T.M.; Rodrigues, W.P.; Netto, A.T.; Reis, F.D.; Peçanha, A.L.; de Assis Figueiredo, F.A.M.M.; de Sousa, E.F.; Glenn, D.M.; Campostrini, E. Comparison between single-leaf and whole-canopy gas exchange measurements in papaya (*Carica papaya* L.) plants. *Sci. Hortic.* **2016**, *209*, 73–78. [[CrossRef](#)]
12. Liu, J.; Hu, T.T.; Fang, L.; Peng, X.Y.; Liu, F.L. CO₂ elevation modulates the response of leaf gas exchange to progressive soil drying in tomato plants. *Agric. For. Meteorol.* **2019**, *268*, 181–188. [[CrossRef](#)]
13. Baldocchi, D.D. A comparative study of mass and energy exchange rates over a closed C3 (wheat) and an open C4 (corn) crop: II. CO₂ exchange and water use efficiency. *Agric. For. Meteorol.* **1994**, *67*, 291–321. [[CrossRef](#)]
14. Law, B.E.; Falge, E.; Gu, L. Environmental controls over carbon dioxide and water vapor exchange of terrestrial vegetation. *Agric. For. Meteorol.* **2002**, *113*, 97–120. [[CrossRef](#)]
15. Montagnani, L.; Zanotelli, D.; Tagliavini, M.; Tomelleri, E. Timescale effects on the environmental control of carbon and water fluxes of an apple orchard. *Ecol. Evol.* **2018**, *8*, 416–434. [[CrossRef](#)]
16. Vialet-Chabrand, S.; Matthews, J.S.A.; Brendel, O.; Blatt, M.R.; Wang, Y.; Hills, A.; Griffiths, H.; Rogers, S.; Lawson, T. Modelling water use efficiency in a dynamic environment: An example using *Arabidopsis thaliana*. *Plant Sci.* **2016**, *251*, 65–74. [[CrossRef](#)]
17. Gowik, U.; Brautigam, A.; Weber, K.L.; Weber, A.P.; Westhoff, P. Evolution of C4 photosynthesis in the genus flaveria: How many and which genes does it take to make C4? *Plant Cell* **2011**, *23*, 2087–2105. [[CrossRef](#)]
18. Buckley, T.N.; Sack, L.; Farquhar, G.D. Optimal plant water economy. *Plant Cell Environ.* **2017**, *40*, 881–896. [[CrossRef](#)]
19. Yu, Q.; Zhang, Y.Q.; Liu, Y.F.; Shi, P.L. Simulation of the stomatal conductance of winter wheat in response to light, temperature and CO₂ changes. *Ann. Bot.* **2004**, *93*, 435–441. [[CrossRef](#)]
20. Vuichard, N.; Ciais, P.; Viovy, N.; Li, L.H.; Ceschia, E.; Wattenbach, M.; Bernhofer, C.; Emmel, C.; Grünwald, T.; Jans, W.; et al. Simulating the net ecosystem CO₂ exchange and its components over winter wheat cultivation sites across a large climate gradient in Europe using the ORCHIDEE-STICS generic model. *Agric. Ecosyst. Environ.* **2016**, *226*, 1–17. [[CrossRef](#)]
21. Tong, X.J.; Li, J.; Yu, Q. Ecosystem water use efficiency in an irrigated cropland in the North China Plain. *J. Hydrol.* **2009**, *374*, 329–337. [[CrossRef](#)]
22. Cleverly, J.; Vote, C.; Isaac, P. Carbon, water and energy fluxes in agricultural systems of Australia and New Zealand. *Agric. For. Meteorol.* **2020**, *287*, 107934. [[CrossRef](#)]
23. Lin, Y.S.; Medlyn, B.E.; Duursma, R.A.; Prentice, I.C.; Wang, H.; Baig, S.; Eamus, D.; de Dios, V.R.; Mitchell, P.; Ellsworth, D.S.; et al. Optimal stomatal behaviour around the world. *Nat. Clim. Chang.* **2015**, *5*, 459–464. [[CrossRef](#)]
24. Buckley, T.N.; Mott, K.A. Modelling stomatal conductance in response to environmental factors. *Plant Cell Environ.* **2013**, *36*, 1691–1699. [[CrossRef](#)] [[PubMed](#)]
25. French, R.; Schultz, J. Water use efficiency of wheat in a Mediterranean-type environment. I. The relation between yield, water use and climate. *Aust. J. Agric. Res.* **1984**, *35*, 743–764. [[CrossRef](#)]
26. Rad, M.H.; Sarkheil, H.; Khojastehpour, R. Analysing water use efficiency and productivity in Iran’s metropolises. *Proc. Inst. Civ. Eng. Water Manag.* **2019**, *172*, 102–108.
27. Gobbett, D.L.; Hochman, Z.; Horan, H.; Garcia, J.N.; Grassini, P.; Cassman, K.G. Yield gap analysis of rainfed wheat demonstrates local to global relevance. *J. Agric. Sci.* **2017**, *155*, 282–299. [[CrossRef](#)]
28. Slafer, G.A.; Rawson, H.M. Base and optimum temperatures vary with genotype and stage of development in wheat. *Plant Cell Environ.* **1995**, *18*, 671–679. [[CrossRef](#)]
29. Fitsum, T.; Haimanote, B.; Bruce, S.; Yiannis, A.; Gerrit, H.; Aditya, S. Exploring deficit irrigation as a water conservation strategy: Insights from field experiments and model simulation. *Agric. Water Manag.* **2023**, *289*, 108490.

Disclaimer/Publisher’s Note: The statements, opinions and data contained in all publications are solely those of the individual author(s) and contributor(s) and not of MDPI and/or the editor(s). MDPI and/or the editor(s) disclaim responsibility for any injury to people or property resulting from any ideas, methods, instructions or products referred to in the content.